PARTICLE SALTATION DOWN A SLOPING PLANE

KIAN CHUN QUA, ZHI-QIAN WANG, NIAN-SHENG CHENG

School of Civil and Environmental Engineering, Nanyang Technological University, 50 Nanyang Avenue, Singapore 639798

Saltation of sediment particles is an important phenomenon for bedload transport. Such phenomena are examined in this study by investigating particle motion along a sloping plane. A series of experiments are conducted in a stagnant water environment, where sediment particle motion is driven solely by gravity, by varying particle size and slope angle. Experimental observations are also compared with analytical results derived based on the force equilibrium consideration. Implications of the present study for sediment transport are finally discussed.

1 Introduction

Due to numerous factors involved, it is almost impossible to predict exactly the movement of a particle that is transported by water either as suspended load or bedload. Some of these factors include speed of river flow, riverbed conditions, sediment size, the presence of other particles, gradient of riverbed, etc.

In order to better understand nature, researchers have since created numerous models to study river flow. Simplified models are often used to study the relationship among some of the parameters before one can fully comprehend the bigger picture (Francis 1973). By understanding motion of single particles and their velocity, we will then be able to understand the amount of sediment that can be transported downstream and to better manage the situation.

In this study, a no-flow condition was created to study the movement of a particle purely via gravity, buoyancy effect and friction down a simulated riverbed. The relationship among these three parameters will then be studied to provide some insight to sediment transport in the flow system of a river.

2 Force Equilibrium for A Particle Falling Down A Slope

When a particle falls/slides/jumps down a slope, it is subjected to three forces in the slope direction as shown in figure 1, assuming that the particle is submerged in a stagnant water environment. They are:

a) Component of gravity (submerged weight):

$$W \sin \theta \tag{1}$$

b) Drag

$$F_D = C_D \frac{u_p^{\ 2}}{2g} \frac{\pi d^2}{4} \rho g \tag{2}$$

c) Friction

$$F_S = fW \cos\theta \tag{3}$$

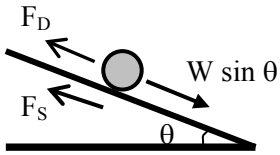

Figure 1. Forces acting on a particle along a slope

Here, W is the submerged weight of the particle, θ is the slope angle, C_D is the drag coefficient, u_p is the average velocity at which the particle moves down the slope, d is the mean diameter of the particle, ρ is the fluid density, g is the gravitational acceleration, and f is the friction factor. It is also assumed that the particle is spherical in shape and an equilibrium velocity achieves quickly when the particle moves in water. Furthermore, the downslope component of the gravitational force can be also defined using a nominal shear stress,τ, or the corresponding shear velocity, u_* ($=\sqrt{\tau/\rho}$), which yields

$$W \sin\theta \equiv \tau \frac{\pi d^2}{4} \equiv \rho u_*^2 \frac{\pi d^2}{4} \tag{4}$$

The use of τ and u_* is convenient when comparing the results presented in this study with those associated with bedload transport. Since $W = (\rho_s - \rho)g\pi d^3/6$ where ρ_s is the particle density, Eq. (4) can be re-written as

$$\tau_* = \frac{u_*^2}{\Delta g d} = \frac{\sin\theta}{1.5} \tag{5}$$

where $\Delta = (\rho_S - \rho)/\rho$ and τ_* is the dimensionless shear stress. Now, consider force equilibrium along the slope, i.e.

$$F_D + F_S = W \sin\theta \tag{6}$$

Substituting Eqs. (2) and (3) into Eq. (6), we get

$$C_D \frac{u_p^2}{2g} \frac{\pi d^2}{4} \rho g = W \sin\theta - W \cos\theta . f \tag{7}$$

Using Eq. (5), Eq. (7) can be further expressed as

$$C_D \frac{u_p^2}{2g} \frac{\pi d^2}{4} \rho g = W(1.5\tau_*) - fW\sqrt{1 - 2.25\tau_*^2} \tag{8}$$

or

$$u_{p^*} = \frac{u_p}{\sqrt{\Delta g d}} = \sqrt{\frac{4}{3C_D}} \cdot \sqrt{1.5\tau_* - f\sqrt{1 - 2.25\tau_*^2}} \tag{9}$$

Note that the drag coefficient for nature sediment and spherical particles are different. They are generally related to the Reynolds number, Re (= $u_p d/\nu$), and may be estimated using the following two equations.

For natural sediment (Cheng 1997),

$$C_D = \left[\left(\frac{32}{\mathrm{Re}} \right)^{\frac{1}{n}} + 1 \right]^n \qquad \text{where n = 1.5} \tag{10}$$

For spherical particles,

$$C_D = \left[\left(\frac{24}{\mathrm{Re}} \right)^{\frac{1}{m}} + 0.53 \right]^m \qquad \text{where m = 2} \tag{11}$$

For the experiments conducted, the viscosity of the water was 0.8 x 10^{-6} m^2/s.

3 Experimental Setup

Four different planes with surfaces roughened by various sediment particles were used to simulate different riverbed. Each plane was made from perspex with dimension of 1000mm by 600mm by 10mm. The setup of the tank is shown in Figure 2. A horizontal plank was placed across tank where particles were allowed to fall freely from the end of the plank, which was close to the plane.

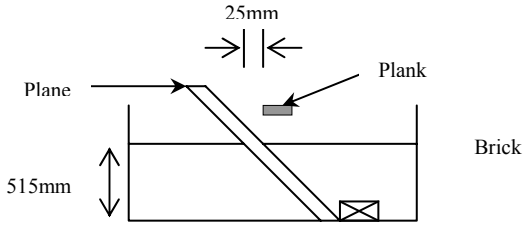

Figure 2. Side view of experimental setup

The particles were dropped from the plank at the side nearer to the plane. By allowing the free fall of the particles, the possible interference by human from releasing from the hand was eliminated. Moreover, the initial velocity would be consistent with this setup where all the different materials/sand particles were released from the same point.

Movement of the particles down the slope was filmed midway from the water level. This was to ensure that the particles attained constant velocity before the reading of the velocity was taken. A total of 5 different slope angles (namely 48^0, 51^0, 54^0, 57^0, 60^0) were set for the experiment. Five different particles were used as well, namely red sand particles, brown sand particles, grey sand particles, and glass balls of 3mm and 5mm diameter.

All the planes were set up in the 5 different angles for the experiment, though not all the 5 particles were dropped onto the 4 different planes. For the smooth plane and the plane covered by the red particles (called red plane), all the particles were dropped and studied as the size of the settling particles were larger than that of the particle covering the plane. In the case of the planes covered by brown and grey particles (called brown and grey planes, respectively), only the 5mm glass balls, brown and grey particles were studied. The 3mm glass balls and red particles were too small in diameter and they got easily stuck in between the larger particles before they could move down the plane.

4 Experimental Results

The size distributions of the sediments used are shown in Figure 3. The other properties are summarized in Table 1.

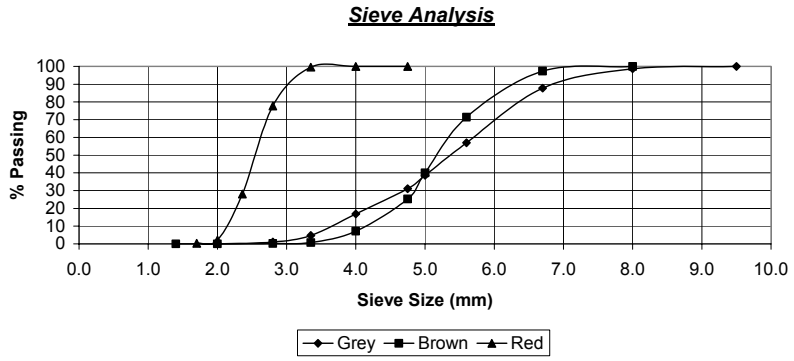

Figure 3. Sieve analysis

The shape factor is calculated using the following formula

$$SF = \frac{c}{\sqrt{ab}} \tag{12}$$

where a, b and c are the maximum, intermediate and minimum lengths of the particle's diameter respectively. The angle of repose for a particular particle was measured in the open air and also in water.

Table 1. Properties of particles used for experiment

	Mean Diameter	Shape Factor	Density (kg/m^3)	Angle of Repose	
				Wet	Dry
3mm particle	3.12	-	2639.30	-	-
5mm particle	4.16	-	2571.10	-	-
Red particle	2.55	0.621	2222.73	37.7^0	37.4^0
Brown particle	5.15	0.685	2515.58	35.8^0	34.8^0
Grey particle	5.35	0.576	2663.12	33.2^0	31.65^0

Figures 4-7 show that the particle saltation velocity generally varies with the slope angle, and the characteristics of particle and sloping plane. The velocity used for plotting is the value averaged using 10 readings for each test.

Figure 4. Average downslope velocity measured for glass beads (3mm, 5mm), red, brown and grey particle saltating along smooth plane.

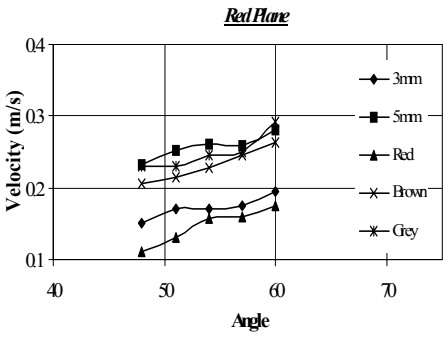

Figure 5. Average downslope velocity measured for glass beads (3mm, 5mm), red, brown and grey particle saltating along red plane.

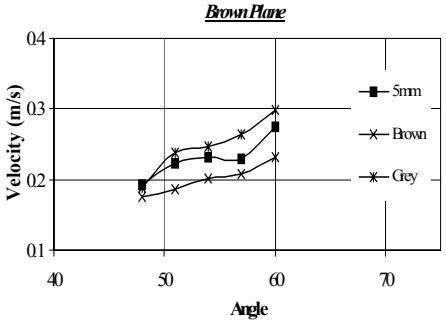

Figure 6. Average downslope velocity measured for glass beads (5mm), brown and grey particle saltating along brown plane.

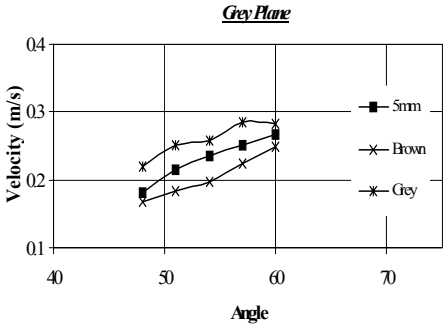

Figure 7. Average downslope velocity measured for glass beads (5mm), brown and grey particle saltating along grey plane.

4.1. *Factors Affecting Saltation Velocity*

Based on Figures 4-7, some observations can be made, as detailed below.

- A particle with higher density has larger saltation velocity. This is expected as a particle with higher density is heavier and thus falls faster.
- The particles move down a plane faster at a larger angle.
- With the plane covered by relatively larger particles, more pores exist in between particles, resulting in more energy lost as particles move across them. Thus, the velocity can be seen to be slower in Figure 6 and Figure 7. These two figures also show that the larger the moving particle, the faster it moves across the plane.
- In Figure 5, a clear indication can be seen where the velocity of the 5mm glass bead, brown and grey particles are very much similar while that of the 3mm and red particles are much slower. This may be due to the relative size of the saltating particles. Sketches given in Figures 8 and 9 show that moving particle may experience difficulties when rolling across the surface roughened by larger particles.

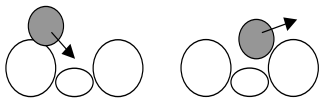

Figure 8. Smaller particle moving across relatively larger particles

Figure 9. Larger particle moving across relatively smaller particles

♦ Finally, comparing Figure 4 for the smooth plane with Figure 5 for the rough plane, the velocity of the particles is reduced due to friction.

4.2. *Comparison of Measured and Calculated Velocity*

To compare the theoretical computation with the actual measured velocity, we first consider the situation with $u_{p*} = 0$. For this critical condition, the corresponding shear stress is denoted as τ_{*c}, which is related to the friction factor. Applying condition of $u_{p*} = 0$ to Eq. (9) yields

$$\sqrt{1.5\tau_{*C} - f\sqrt{1-2.25\tau_{*C}^2}} = 0 \tag{13}$$

or

$$f = \frac{1.5\tau_{*C}}{\sqrt{1-(1.5\tau_{*C})^2}} \tag{14}$$

Substituting Eq. (14) in to Eq. (9) and manipulating, we get

$$\frac{u_p}{u_*} = \sqrt{\frac{2}{C_D}}\sqrt{1-\frac{\tau_{*C}}{\tau_*}}\sqrt{\frac{1-(1.5\tau_*)^2}{1-(1.5\tau_{*C})^2}} \tag{15}$$

In the following, Eq. (15) is used for computing the saltation velocity, where τ_{*c} can be related to the angle of repose by assuming

$$f = \tan\alpha \tag{16}$$

where α = angle of repose. It should be mentioned that the saltation velocity for the 3mm and 5mm glass beads were not calculated due to difficulty in determining their angles of repose.

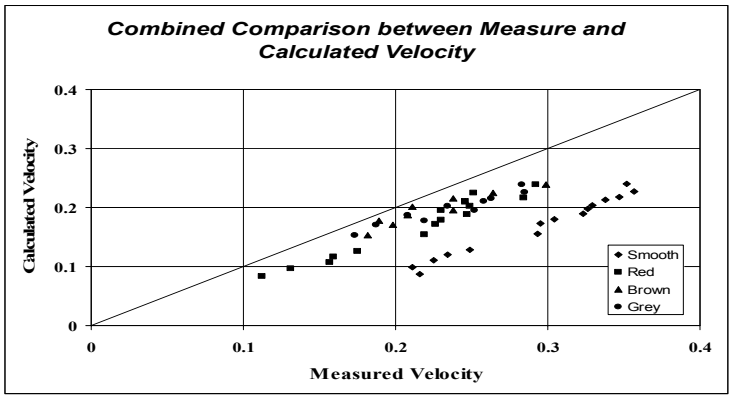

Figure 10. Combined comparison between measured and calculated velocity

Figure 10 shows a combined comparison between the computed and measured saltation velocities. Generally, the computed velocities are smaller. The differences between the measured and calculated velocities for the red, brown and grey planes are approximately 22.5%, 12.8% and 15.8% respectively. The average difference between the velocities is 13%.

The differences are induced by several factors. Generally, with the higher saltation velocity, the less frequently the moving particle contacts the sloping plane. This may imply that a smaller friction factor should be used for the computation, and thus the resultant computed velocity would be larger. Furthermore, if the friction factor is very small, the saltation velocity will be proportional to the shear velocity, as suggested by Eq. (9). In other words, the saltation velocity computed based on the angle of repose would be more reasonable for the slower saltation stage.

As an initial inertia was given to each particle in the experiment to allow the particle to roll down the plane, this might be another reason for the difference induced. The inertia could result in an increase in the measured saltation velocity. The difference observed might be also caused by uncertainties associated with the drag coefficient, C_D, which was estimated using the empirical formulas. It is also noted that as the particle moves down the plane, it does not move in a straight line. This phenomenon is not taken into account for the theoretical derivation. Collision is another complicated but important issue worthy of further investigation. How to include the collision effect in the formulation is not clear.

In Figures 11-14, the dimensionless saltation velocity, u_{p*}, is plotted against the dimensionless shear stress. The latter is commonly used in sediment transport. From the figures, it follows that the relationship between u_{p*} and τ_* seems linear. However, more data are required in the lower region to substantiate this argument. For the cases of the smooth and red planes, the results show that the u_{p*} value for the 5mm beads is relatively higher. For the case of the 3mm beads, the u_{p*} value is relatively close to the others.

5 Conclusion

Due to the many factors intervening in the process of sediment transport in a river, the only way to better understand the complex process is to single out a few important parameters and then to explore the relationship among them.

The saltation of a particle along a sloping plane was measured and then compared with theoretical formula derived based on force equilibrium. Though this formula does not take all the sediment properties into consideration, it predicts saltation velocities that are 20% to 40% lower than the measurements. The experimental data also indicate that the dimensionless saltation velocity may be linearly related to the dimensionless shear velocity.

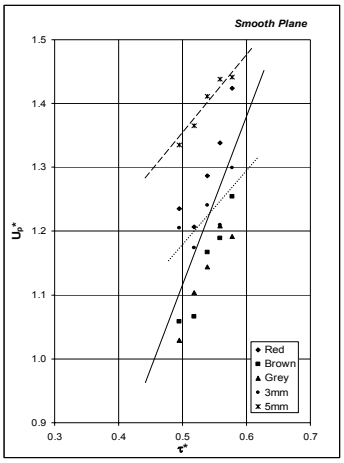

Figure 11 u_{p*} vs τ^* for smooth plane

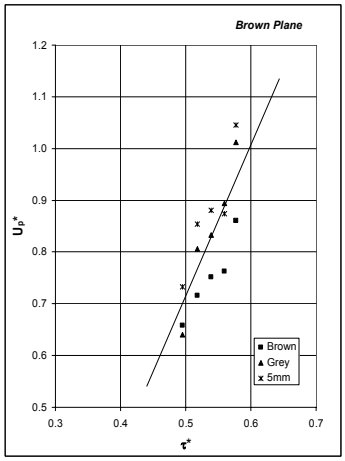

Figure 13 u_{p*} vs τ^* for brown plane

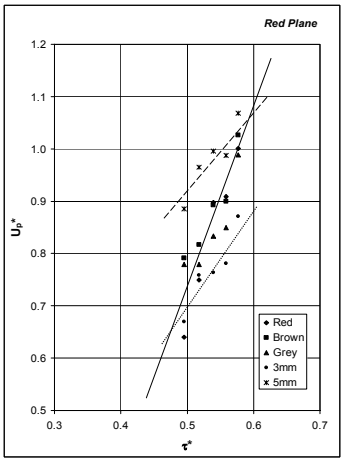

Figure 12 u_{p*} vs τ^* for red plane

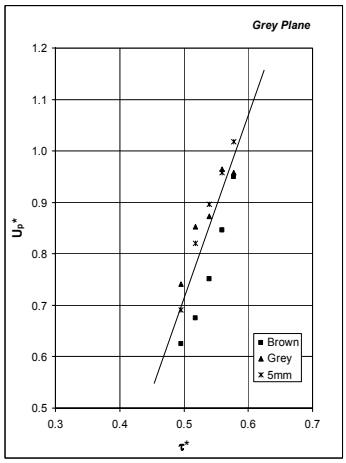

Figure 14 u_{p*} vs τ^* for grey plane

References

Cheng N. S. (1997). "Simplified settling velocity formula for sediment particle." Journal of Hydraulic Engineering, Vol. 123, No. 2, pp 149-152.

Francis J. R. D. (1973) “Experiments on the motion of solitary grains along the bed of a water-stream” Proceedings of the Royal Society of London. Series A, Mathematical and Physical Sciences, Vol. 332 Issue 1591 443-471.